DYNAMICS OF BRAKING OF THE TRANSPORT AND TECHNOLOGICAL TRAIN

Ivan Koliesnik[1], Yevhen Kalinin[1], Juliana Koliesnik[2], Pankova Oksana[3], Vitalii Shutko[4]
[1] National University of life and environmental sciences of Ukraine, Ukraine
[2] State biotechnological university, Ukraine
[3] Kharkiv national automobile & highway university
[4] Sumy National Agrarian University
E-mails: ivankolesnik@nubip.edu.ua, kalinin@nubip.edu.ua, julianakolesnik@nubip.edu.ua, pankova_oksana@ukr.net, v.shutko.gs@snau.edu.ua

Abstract - The work examines the interaction of the links of the transport-technological train during braking, which occur in the traction-coupling device. The influence of these forces on the braking properties of the transport-technological train and its dynamics as a whole is analyzed. The change in the processes that take place during the braking of the transport-technological train is considered, taking into account the presence of an elastic connection at the coupling point.
It is noted that the operation of the traction-coupling device is largely determined by the presence of damping at the connection point, which is caused by wear and deformation of the coupling elements.
The theoretical change of the processes occurring during the braking of the transport-technological train is described.
Determine the normal reactions acting on the axle of the tractor and trailer during braking. A system under the influence of active efforts and connection reactions was considered, replacing the action of connections with their reactions.

Keywords: Transport-technological unit, Dynamics, Braking, Tractor, Trailer.

1. Introduction

Altomonte Andrea in this work, an exhaustive performance analysis is conducted on the heavy-duty Diesel engine of a yard tractor used in port logistics, in order to estimate the potential of regenerative braking, which could be exploited in an electrified vehicle configuration. To this aim, experimental measurements are carried out at the dynamic test bench with reference to peculiar duty cycles, retrieved from an on-field measurement campaign. The on-field data are collected by means of a custom instrumentation, designed to gather real-time data from the CAN bus system of a yard tractor, equipped with the same engine, operating in the port of Salerno, Italy [1].

Hesham Rakha is considering model uses these variables to construct synthetic drive cycles for each roadway segment and then predicts average fuel consumption and emission rates for four modes: decelerating, idling, accelerating, and cruising. Within each mode of operation, fuel consumption and emission rates are determined using relationships that are derived from instantaneous microscopic energy and emission models. The model allows the user to calibrate two additional input parameters, namely typical deceleration and acceleration rates. The proposed model is demonstrated to success-fully predict fuel consumption and hydrocarbon, carbon monoxide, carbon dioxide, and oxides of nitrogen emission rates [2].

Karol Tucki paper presents a computer tool that uses neural networks to simulate driving tests. Data obtained from tests on the Mercedes E350 chassis dynamometer were used for the construction of the neural model. for the built model, were used to create simulation control runs for driving tests. As a result of the processing of this same computer tool, mass consumption of fuels and CO2 emissions were analyzed in driving tests for the given analyzed vehicle [3].

Felez Jesus based on the latter, the fundamental motivation of this paper has been to provide “intelligence” to the articulated vehicles in order to convert it into an autonomous vehicle. This can be obtained from the development of a control system based on predictive model control (MPC). From this control system it is intended that the vehicle by itself can carry out the usual driving maneuvers, achieving the adaptation of the vehicle to a previously fixed path. In addition, it is intended to introduce a stability control to the articulated vehicle to avoid its instability under high speeds and forced trajectories.

This steering stability control will be based on differential braking [4].

Borawski Andrzej in this manuscript tried to check how the brakes of a semi-trailer heat up during emergency braking. For this, a mathematical model of the braking process was developed and simulation tests were carried out for different initial speeds and different loads. The results are friction material temperature profiles that show how the drum and brake pads heat up during braking and cool down immediately after stopping [5].

In Samorodov Vadim's article, the given description of the criteria is used to form changes in the control parameters of hydraulic machines (hydraulic pump and hydraulic motor) in the process of acceleration and braking of a wheeled tractor. A rational change of hydraulic machine control parameters at the stages of acceleration and braking for a wheeled tractor with stepless hydrovolume mechanical transmission, which is carried out according to the output differential scheme, has been formed. During the study of the obtained dependence of hydraulic machine regulation parameters, the change of such indicators as acceleration and braking time was determined; braking distance of a wheeled tractor; Efficiency of hydrovolumetric drive and hydrovolumetric mechanical transmissions; the working pressure difference in the hydraulic actuator. It was established that when using a rational change of hydraulic machine control parameters instead of a linear one at the stages of acceleration and braking, the zone of the highest value of the coefficient of useful action of hydrovolumetric-mechanical transmission narrows, which, in turn, indicates the load of the hydraulic branch of the hydrovolume transmission [6].

Xu Shiwei this work proposes a multi-mode composite braking control strategy for the five-axle distributed electric wheel-drive heavy-duty vehicle. Firstly, given the differences in braking dynamics between two-axle vehicles and multi-axle vehicles, the brake dynamics characteristics of multi-axle vehicles are analyzed, and the vehicle dynamics model of multi-axle vehicles is constructed. Next, a multi-mode composite braking control strategy including a fully electric braking state and hybrid electro–hydraulic braking state is proposed in order to improve the braking energy recovery and braking stability [7].

Wan Zhen's paper discusses the problems of calculating the braking of a multi-axle vehicle, which was based on the classical model and described the general models of the linear braking dynamics of a multi-axle vehicle. The models retain suspension constraints and introduce suspension distortion harmonization equations. Based on the models, general formulas were derived for calculating the vertical opposing force from the road. He then proposed a method to obtain the locking sequence of a multi-axle vehicle, which is easy to implement using computer language, and derived general formulas for calculating braking power, braking acceleration and linear braking stopping distance [9].

Wu Xinping's experimental results show that the time required to achieve the target clamping force in an electronic mechanical brake system using self-disturbance suppression control and PI control is only 0.01s, but there is a problem of excessive control in PI control. -differential system. between 0.12 s and 0.2 s, while the self-interference controller does not have this problem. Meanwhile, no matter the intervention applied, the electronic mechanical braking system with automatic interference suppression control can ensure that the clamping force does not fluctuate [10].

2. State-of-the-Art

An integral part of the dynamics of the transport and technological train is braking, which ensures the safety of traffic on the roads. But despite the importance of this issue, it is currently not given enough attention, as a result of which we often see transport-technological trains on the roads, the brake systems of the component links of which are not coordinated, and the traction-coupling devices are not perfect.

Therefore, the main stage in field conditions for effectively reducing the unsteady motion of the transport-technological train is the improvement of its dynamic system.

Taking into account the peculiarities of the study of the road - tire - suspension - vehicle - operator system, using the magnitude and range of changes of such generalized disturbing indicators of influence as speed, deceleration, time, braking force, it is necessary to determine the change of loads in the traction-coupling device, as well as normal reactions on the axles of the transport-technological unit during braking and the effect of these changes on the braking properties of the unit, taking into account the type of traction-coupling device used.

Using the magnitude and range of changes in such generalized parameters of the disturbing influence as speed, time, force, power, it is necessary to determine the change in loads in the traction-coupling device, normal reactions on the axles of the tractor and trailer during braking, and the effect of these changes on the braking properties of the transport-technological train.

3. Analysis of the Interaction of the Links of the Transport-technological Train During Braking

The interaction of the links of the transport-technological train during braking is characterized by the forces arising in the traction-coupling device. To analyze the influence of these forces on the

braking properties of the transport-technological train and its dynamics in general, consider the change in the processes that take place during the braking of the transport-technological train, taking into account the presence of an elastic connection at the coupling point.

When analyzing the braking process, we will make the following assumptions:

- links of the transport and technological train are considered material points;
- from internal forces, only reactions in the traction-coupling device act on each link of the transport-technological train;
- the engine is disconnected from the transmission and torques are not applied to the wheels of the tractor;
- the road in the transverse direction does not have a slope;
- the centers of gravity of each link of the transport and technological train lie in the longitudinal plane of symmetry;
- the braking forces applied at each moment of braking with a constant coefficient of tire adhesion to the road correspond to the forces that can be transmitted through the wheel, taking into account the weight falling on it and the coefficient of adhesion to the road.

It should be noted that the operation of the traction-coupling device is largely determined by the presence of damping at the connection point, which is caused by wear and deformation of the coupling elements.

We will describe theoretically the change in the processes that occur when the transport-technological train is braked. Let the system (Fig. 1), which moves by inertia with the initial speed υ0, at some point in time apply braking forces P_{T_TP} (for the tractor) and $P_{п\_TP}$ (for the trailer). At the same time, the ratio of forces is such that the deceleration of the j_{TP} tractor is greater than the deceleration of the j_{TP} trailer.

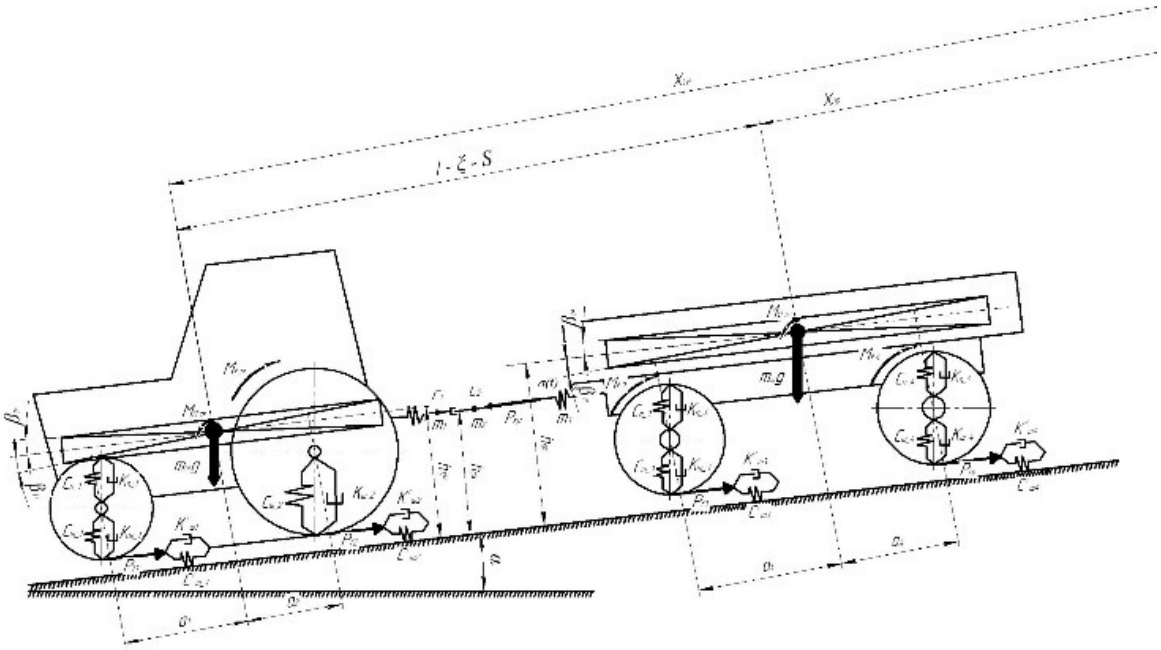

Figure 1: Diagram of a dynamic model of braking of a transport-technological train

In accordance with the above assumptions and features, we will write down the system of equations (1 – 8) and after solving it, we will get the damping function, with the help of which we will consider the effect of the connection on the change in the traction force during the braking of the transport and technological train [8, 12, 22].

At $0 \le t \le t^{/}$:

$$\begin{cases} m_{tr}\ddot{x}_{tr} = -P_{tr} + \sigma\dot{S}_3 \\ m_{pr}\ddot{x}_{pr} = -P_{pr} - \sigma\dot{S}_3 \\ m_3\ddot{S}_3 = 4c_d v_{ж} l_d \gamma_{ж} F_d^2 \dot{S}_3 / (\pi d_4)^{-\sigma\dot{S}_3} \\ x_{tr} = x_{pr} + S_3 + l + \zeta \end{cases} \quad (1)$$

At $t \ge t^{/}$:

$$\begin{cases} m_{tr}\ddot{x}_{tr} = -P_{pr} + \sigma^{/}\dot{S}_3 \\ m_{pr}\ddot{x}_{pr} = -P_{pr} - \sigma^{/}\dot{S}_3 \\ m_3\ddot{S}_3 = 4c_d v_{ж} l_d \gamma_{ж} F_d^{/2} \dot{S}_3 / (\pi d_4)^{-\sigma^{/}\dot{S}_3} \\ x_{tr} = x_{pr} + S_3 + l + \zeta \end{cases} \quad (2)$$

Multiplying equation (1) by $m_{ПР}$, and equation (2) by m_{TP}, we find the difference of the resulting equations:

$$\ddot{x}_{tr}-\ddot{x}_{pr}=-\frac{P_{tr}m_{pr}}{m_{tr}m_{pr}}+\frac{P_{pr}m_{tr}}{m_{tr}m_{pr}}+ +\left(\frac{m_{pr}}{m_{tr}m_{pr}}+\frac{m_{tr}}{m_{tr}m_{pr}}\right)\sigma\dot{S}_3 \quad (3)$$

Denoting $\sigma_0=4c_d v_{ж} l_d \gamma_{ж} F_d^2 \dot{S}_3/(\pi d_4)$, and we express from equation (1)

$$\sigma S_3=\sigma_0\dot{S}_3-m_3\ddot{S}_3 \quad (4)$$

Let's substitute equation (4) in (3)

$$\ddot{S}_3=\frac{P_{t\_pr}m_{tr}-P_{t\_tr}m_{pr}}{m_{tr}m_{pr}}- -\left(\frac{m_{tr}+m_{pr}}{m_{tr}m_{pr}}\right)\left(\sigma_0\dot{S}_3-m_3\ddot{S}_3\right) \quad (5)$$

Let's enter the notation:

$k_m=\frac{m_{tr}+m_{pr}}{m_{tr}m_{pr}}$ – coefficient of weight characteristic;

$j_S=\frac{P_{t\_pr}m_{tr}-P_{t\_tr}m_{pr}}{m_{tr}m_{pr}}$ – relative deceleration of links of the transport and technological train;

$j_{sm}=\frac{j_S}{1-k_m m_3}$ – relative deceleration of the links taking into account the inertia of the traction-coupling device;

$2E_0=\frac{k_m\sigma_0}{1-k_m m_3}$ – constant fading.

Let's rewrite equation (5) in the form:

$$\ddot{S}_3+2E_0\dot{S}_3=j_{sm} \quad (6)$$

Let's rewrite equation (6) as the initial conditions: *t=0, S₃=0,* $\dot{S}_3=\vartheta_{0\xi}$

$$\dot{S}_3=\left(\frac{j_{sm}}{4E_0^2}-\frac{\vartheta_{0\xi}}{2E_0}\right)e^{-2ht}+\frac{j_{sm}}{2E_0}t- -\left(\frac{j_{sm}}{4E_0^2}-\frac{\vartheta_{0\xi}}{2E_0}\right) \quad (7)$$

Transforming equation (7), we get

$$S_3=\frac{j_S}{k_m\sigma_0}t+\frac{(1-k_m m_3)(j_S-\vartheta_{0\xi}k_m\sigma_0)}{(k_m\sigma_0)^2}\cdot \cdot\left(e^{\frac{k_m\sigma_0}{1-k_m m_3}t}-1\right) \quad (8)$$

Let's determine the resistance of the elastic connection. For this we will find $\dot{S}_3$ and $\ddot{S}_3$.

$$\dot{S}_3=\frac{j_S}{k_m\sigma_0}-\frac{(j_S-\vartheta_{0\xi}k_m\sigma_0)}{k_m\sigma}e^{-\frac{k_m\sigma_0}{1-k_m m_3}t} \quad (9)$$

$$\ddot{S}_3=\frac{(j_S-\vartheta_{0\xi}k_m\sigma_0)}{1-k_m m_3}e^{-\frac{k_m\sigma_0}{1-k_m m_3}t} \quad (10)$$

Expressing σ from equation (4) and substituting (9) and (10) into the resulting equation, we get:

$$\sigma=\sigma_0-\frac{k_m m_3\sigma_0(j_S-\vartheta_{0\xi}k_m\sigma_0)e^{-\frac{k_m\sigma_0}{1-k_m m_3}t}}{(1-k_m m_3)\left(j_S-(j_S-\vartheta_{0\xi}k_m\sigma_0)e^{-\frac{k_m\sigma_0}{1-k_m m_3}t}\right)} \quad (11)$$

Let's find the force arising in the connection $P_э$

$$P_э=\sigma\dot{S}_3 \quad (12)$$

or

$$P_э=\frac{j_S(1-k_m m_3)-(1-k_m m_3+m_3)(j_S-\vartheta_{0\xi}k_m\sigma_0)e^{-\frac{k_m\sigma_0}{1-k_m m_3}t}}{k_m(1-k_m m_3)} \quad (13)$$

The resulting formula (13) can be used to calculate the force in a hydrohook of standard construction. To obtain a formula that can be used in connection calculations, it is necessary to solve the system of equations (2). It is solved similarly to the system of equations, (1).

The initial conditions on the site are as $t\geq t'$ follows: $t=t'.S_3=S_3(t'),\dot{S}_3=\vartheta(t')$

Let's enter the notation:

$\sigma_0'=4c_d v\ l_d\gamma\ F_d'^2\dot{S}_3/(\pi d_4)$ – constant resistance to sections $t\geq t'$;

$2E_0'=\frac{k_m\sigma_0'}{1-k_m m_3}$ – constant decline in the area $t\geq t'$.

Similar to the solved system of equalities (1), a differential equalization of a different order is obtained:

$$\ddot{S}_3+2E_0'\dot{S}_3=j_{Sm} \quad (14)$$

The solution to equation (14) under the initial conditions of the site has the form:

$$S_3=\frac{j_{sm}}{2E_0'}(t-t')+\frac{\vartheta(t')}{2E_0'}\left(1-e^{-2E_0'(t-t')}\right)+ +\frac{j_{sm}}{4E_0'^2}\left(e^{-2E_0'(t-t')}-1\right)+S_3(t') \quad (15)$$

After transforming equation (15), we obtain:

$$S_3=\frac{j_S}{k_m\sigma_0'}(t-t')+\frac{\vartheta(t')(1-k_m m_3)}{k_m\sigma_0'}\left(1-e^{\frac{k_m\sigma_0'}{1-k_m m_3}t(t-t')}\right)+ +\frac{j_S(1-k_m m_3)}{(k_m\sigma_0')}\left(e^{\frac{k_m\sigma_0'}{1-k_m m_3}t(t-t')}-1\right)+S_3(t') \quad (16)$$

Let's write down the first and second derivatives of S3:

$$\dot{S}_3=\frac{j_S}{k_m\sigma_0'}+\left(\vartheta(t')-\frac{j_S}{k_m\sigma_0'}\right)e^{\frac{k_m\sigma_0'}{1-k_m m_3}t(t-t')} \quad (17)$$

$$\ddot{S}_3 = \frac{j_S - \vartheta\left(t^{/}\right)k_m\sigma_0^{/}}{1-k_m\sigma_0^{/}} e^{\frac{k_m\sigma_0^{/}}{1-k_m m_3}t\left(t-t^{/}\right)} \quad (18)$$

Expressing σ/ from equation (2) and substituting into the resulting equations (17) and (18), we obtain:

$$\sigma^{/} = \sigma_0^{/} = -\frac{k_m m_3\sigma_0^{/}\left(j_S - \vartheta\left(t^{/}\right)k_m\sigma_0^{/}\right)e^{\frac{k_m\sigma_0^{/}}{1-k_m m_3}t\left(t-t^{//}\right)}}{(1-k_m m_3)\left(j_S - \vartheta\left(t^{/}\right)k_m\sigma_0^{/}\right)e^{\frac{k_m\sigma_0^{/}}{1-k_m m_3}t\left(t-t^{/}\right)}} \quad (19)$$

since

$$P_з = \sigma^{/}\dot{S}_3 \quad (20)$$

where $\dot{S}_3$ - in formula (26) of section $t \ge t^{/}$, then by multiplying the right parts of equations (19) and (17) we get the calculation formula for the force in the connection, which is a damping element, but does not have elastic elements (springs, rubber buffers) in the standard design.

Let's write the system of equations (21) and the system of equations (22). The calculation formulas obtained by solving the first system of equations (21) can be used in the analysis of the operation of traction-coupling devices that include various damping elements in their design. In turn, the same formulas can be used when obtaining the initial conditions for the second system of equations (22), the calculation formulas obtained during the solution of which are more general and can be used in research, can be used when analyzing the operation of traction-coupling devices in any - what design [11, 13, 16].

At $0 \le t \le t^{/}$:

$$\begin{cases} m_{tr}\ddot{x}_{tr} = -P_{tr} + c_{1,2}S + \sigma\dot{S} \\ m_{pr}\ddot{x}_{pr} = -P_{pr} - c_{1,2}S - \sigma\dot{S} \\ m_3\ddot{S} = 4c_d v_j l_d \gamma_j F_d^2 \dot{S}_3 / \left(\pi d_4\right)^{-\sigma\dot{S}} \\ x_{tr} = x_{pr} + S + l + \xi \end{cases} \quad (21)$$

At $t \ge t^{/}$:

$$\begin{cases} m_{TP}\ddot{x}_{TP} = -P_{TP} + c_{1,2}S + \sigma^{/}\dot{S} \\ m_{ПР}\ddot{x}_{ПР} = -P_{ПР} - c_{1,2}S - \sigma^{/}\dot{S} \\ m_3\ddot{S} = 4c_d v_{ж} l_d \gamma_{ж} F_d^{/2} \dot{S}_3 / \left(\pi d_4\right)^{-\sigma^{/}\dot{S}} \\ x_{TP} = x_{ПР} + S + l + \xi \end{cases} \quad (22)$$

Let's solve the system of equations (21). Let's multiply equations (21) by m_{pr} and m_{tr}, respectively, and expressing $\ddot{x}_{tr}$ and $\ddot{x}_{pr}$ writing down their difference:

$$\ddot{x}_{tr} - \ddot{x}_{pr} = \frac{P_{t\_pr}m_{tr} - P_{t\_tr}m_{pr}}{m_{tr}m_{pr}} - \frac{c(m_{tr}+m_{pr})}{m_{tr}m_{pr}}S - \frac{\sigma(m_{TP}+m_{ПР})}{m_{tr}m_{pr}}\dot{S}. \quad (23)$$

From equation (21):

$$\ddot{S}_{TP} - \ddot{S}_{ПР} = \ddot{S} \quad (24)$$

From equation (22):

$$\sigma\dot{S} = \sigma_0\dot{S} - m_3\ddot{S}. \quad (25)$$

Substituting the right-hand parts of equations (24) and (25):

$$\ddot{S} = j_S - \gamma^2 S - k_m\left(\sigma_0\dot{S} - m_3\ddot{S}\right), \quad (26)$$

where $\gamma^2 = \frac{c_{1,2}\left(m_{TP}+m_{ПР}\right)}{m_{TP}m_{ПР}}$ is the circular frequency of natural oscillations.

Let's transform equation (26):

$$\ddot{S} + \frac{k_m\sigma_0}{1-k_m m_3}\dot{S} + \frac{\gamma^2}{1-k_m m_3}S = \frac{j_S}{1-k_m m_3} \quad (27)$$

Let's rewrite equation (27) taking into account the accepted notations:

$$\ddot{S} + 2E\dot{S} + \wp_u^2 S = j_{sm} \quad (28)$$

where $\wp_u^2 = \frac{\gamma^2}{1-k_m m_3}$ is the circular frequency of natural oscillations, taking into account the inertia of the traction coupling device.

The solution of the second-order differential equations (28) has the form:

$$S = \frac{j_{sm}}{\wp_u^2} + U_1 e^{-Et}\sin\left(U_2 + \sqrt{\wp_u^2 - E^2}t\right). \quad (29)$$

The coefficients U_1 and U_2 are determined from the initial conditions: *t=0, S=0,* $\dot{S} = \vartheta_{0\xi}$. We differentiate equation (29) and introduce the notation: $\mu = \sqrt{\wp_u^2 - E^2}$, we get:

$$\dot{S} = U_1 e^{-Et}\left(\mu\cos\left(U_2 + \mu t\right) - E\sin\left(U_2 + \mu t\right)\right) \quad (30)$$

so,

$$\vartheta_{0\xi} = U_1\left(\mu\cos U_2 - E\sin U_2\right) \quad (31)$$

Let's write equation (21) for the moment of time *t=0*:

$$0 = \frac{j_{sm}}{\wp_u^2} + U_1\sin U_2 \quad (32)$$

We have a system of equations (31) and (32) with respect to U_1 and U_2:

$$\begin{cases} \vartheta_{0\xi} = U_1\left(\mu\cos U_2 - E\sin U_2\right) \\ 0 = \frac{j_{sm}}{\wp_u^2} + U_1\sin U_2 \end{cases}$$

Let's write down the solution of this equation:

$$U_1 = \frac{1}{\wp_u^2\mu}\sqrt{\left(\vartheta_{0\xi}\wp_u^2 - Ej_{sm}\right)^2 + j_{sm}^2\mu^2} \quad (33)$$

$$\sin U_2 = -\frac{j_{sm}^2 \mu}{\sqrt{\left(\vartheta_{0\xi} \wp_u^2 - E j_{sm}\right)^2 + j_{sm}^2 \mu^2}} \quad (34)$$

Let's determine the initial compression resistance of the connection elements. For this we will find $\ddot{S}$:

$$\ddot{S} = U_1 e^{-Et}\left(\begin{matrix}\left(E^2 - \mu^2\right)\sin\left(U_2 + \mu t\right) - 2E\mu\cos\cdot \\ \cdot\left(U_2 + \mu t\right)\end{matrix}\right) \quad (35)$$

Expressing σ from equation (25) and substituting the obtained expression and equations (30) and (35), respectively, we obtain:

$$\sigma = \sigma_0 - m_3 \cdot \cdot \frac{\left(E^2 - \mu^2\right)\sin\left(U_2 + \mu t\right) - 2E\mu\cos\left(U_2 + \mu t\right)}{\mu\cos\left(U_2 + \mu t\right) - E\sin\left(U_2 + \mu t\right)} \quad (36)$$

Let's determine the load $P_{кр}$ for the deformable traction coupling device.

In this case, the load on the traction coupling device consists of the sum of the reactions of the elastic connection and the inelastic resistance of the damper, that is:

$$P_{кr} = P_{pr} + P_{dempf} \quad (37)$$

or

$$P_{кр} = cS + \sigma\dot{S} \quad (38)$$

After some transformations, we get:

$$P_{pr} = j_{sm}\left(k_m - m_3\right) \cdot \cdot \left(1 + \frac{\wp_u}{\mu}\sqrt{\left(\frac{\upsilon_{0\xi}\wp_u}{j_{sm}}\right)^2 - \frac{2\vartheta_{0\xi}E}{j_{sm}}} + 1 \cdot e^{-Et}\sin\left(U_2 + \mu t\right)\right) \quad (39)$$

$$P_{dempf} = \frac{j_{sm}}{\wp_u \mu} \cdot \cdot \sqrt{\left(\frac{\vartheta_{0\xi}\wp_u}{j_{sm}}\right)^2 - \frac{2\vartheta_{0\xi}E}{j_{sm}} + 1 \cdot e^{-Et}\left[2E\mu k_m \cos\left(U_2 + \mu t\right) - \right.} \quad (40)$$
$$\left. - \left(2E^2 k_m - \wp_u^2 m_3\right)\sin\left(U_2 + \mu t\right)\right],$$

then

$$P_{кr} = j_{sm}\left(\left(k_m - m_3\right) + \frac{k_m}{\wp_u \mu}e^{-Et}\sqrt{\left(\frac{\upsilon_{0\xi}\wp_u}{j_{sm}}\right)^2 - \frac{2\vartheta_{0\xi}E}{j_{sm}} + 1}\right) \cdot \quad (41)$$
$$\cdot\left[\cos\left(U_2 + \mu t\right)\right]\left(\mu^2 - E^2\right)\sin\left(U_2 + \mu t\right) + 2E\mu\cos\left(U_2 + \mu t\right)\right])$$

As you know, the largest load peaks occur in the traction-coupling device before the braking forces reach their maximum values. It is important to know the values of these loads, which in some cases should be used as calculations [14, 17, 21].

Differentiating equation (38) with respect to time and equating the right-hand side of the resulting equation to zero, we find expressions for terms containing time *t*.

$$\dot{P}_{pr} = j_{sm}\frac{\wp_u}{\mu}\left(k_m - m_3\right)\sqrt{\left(\frac{\upsilon_{0\xi}\wp_u}{j_{sm}}\right)^2 - \frac{2\vartheta_{0\xi}E}{j_{sm}} + 1} \cdot \quad (42)$$
$$\cdot e^{-Et} \cdot \left[\mu\cos\left(U_2 + \mu t\right) - E\sin\left(U_2 + \mu t\right)\right] = 0$$

where

$$tg\left(U_2 + \mu t\right) = \frac{\mu}{E} \text{ or } \sin\left(U_2 + \mu t\right) = \frac{\mu}{\wp_u} \quad (43)$$

Substituting into equation (38) instead $\sin\left(U_2 + \mu t\right)$ of its value from equation (43), we get the expression for determining P_{np_e}:

$$P_{np\_e} = j_{sm}\left(k_m - m_3\right)\left(1 + e^{-Et}\sqrt{\left(\frac{\upsilon_{0\xi}\wp_u}{j_{sm}}\right)^2 - \frac{2\vartheta_{0\xi}E}{j_{sm}}}\right) \quad (44)$$

Time t is determined from equation (43):

$$t = \frac{1}{\mu}arctg\left(\frac{\vartheta_{0\xi}\mu}{\vartheta_{0\xi}E - j_{sm}}\right) \quad (45)$$

Formula (44) can be used in the calculations of both a traction coupling device and, without taking into account deformations, an elastic-damping traction coupling device.

Similarly, we will determine the traction load peaks for the elastic-damping (deformable) traction-coupling device.

We differentiate equation (41) in time and equate the right-hand side of the resulting equation to zero:

$$\dot{P}_{кr} = j_{sm}\frac{k_m}{\wp_u \mu}\sqrt{\left(\frac{\upsilon_{\xi}\wp_u}{j_{Sm}}\right)^2 - \frac{2\vartheta_{\xi}E}{j_{sm}} + 1 \cdot e^{-Et}} \times \times\left[\begin{matrix}E\left(E^2 - 3\mu^2\right)\sin\left(U_2 + \mu t\right) + \mu\left(\mu^2 - 3E^2\right)\cdot \\ \cdot\cos\left(U_2 + \mu t\right)\end{matrix}\right] = 0, \quad (46)$$

where:

$$\sin\left(U_2 + \mu t\right) = \frac{\mu\left(\mu^2 - 3E^2\right)}{\wp_u^3}, \quad (47)$$

$$\cos\left(U_2 + \mu t\right) = \frac{E\left(3\mu^2 - E^2\right)}{\wp_u^3}, \quad (48)$$

Substitute the right parts of equations (47) and (48) into equation (41):

$$P_{кr\_e} = j_{sm}\left(\left(k_m - m_3\right) + k_m e^{Et}\sqrt{\left(\frac{\upsilon_{0\xi}\wp_u}{j_{sm}}\right)^2 - \frac{2\vartheta_{0\xi}E}{j_{sm}} + 1}\right) \quad (49)$$

The time t for the extreme value of P_{kr_e} is determined from equation (35):

$$t = \frac{1}{\mu}arctg\left(\frac{\vartheta_{0\xi}\mu\left(\mu^2 - 3E^2\right) + 2\mu E j_{sm}}{\vartheta_{0\xi}E\left(3\mu^2 - 3E^2\right) + j_{sm}\left(E^2 - \mu^2\right)}\right). \quad (50)$$

To be able to analyze the braking process of a transport-technological train with a traction-coupling device, taking into account its deformation, it is necessary to solve the system of equations (22).

The initial conditions of the next (second) connection operation section, when $t \geq t'$ are as follows: $t = 0, S = S(t'), \dot{S} = \vartheta(t')$.

According to equation (30), we get:

$$S(t') = \frac{j_{sm}}{\wp_u^2} + U_1 e^{-Et'} \sin\left(U_2 + \sqrt{\wp_u^2 - E^2}t'\right), \quad (51)$$

where U_1 and U_2 are defined (see equations (46) and (47).

According to equation (31), we have:

$$\vartheta(t') = U_1 e^{-Et'}\left(\mu\cos(U_2 + \mu t') - E\sin(U_2 + \mu t')\right). \quad (52)$$

The system of equations (31-34) is similar to the system of equations (21).

As a result, the system of equations (22) is reduced to the differential equation:

$$\ddot{S} = j_S - \gamma^2 S - k_m\left(\sigma_0'\dot{S} - m_3\ddot{S}\right). \quad (53)$$

Further transformations lead to a second-order differential equation:

$$\ddot{S} + 2E'\dot{S} + \wp_u^2 S = j_{sm} \quad (54)$$

The solution of equation (54) has the form:

$$S = \frac{j_{sm}}{\wp_u^2} + U_3 e^{-Et}\sin(U_4 + \mu' t), \quad (55)$$

where $\mu' = \sqrt{\wp_u^2 - E'^2}$.

Let us determine the coefficients U_3 and U_4 from the boundary conditions:

$$\begin{cases} S(t') = \frac{j_{Sm}}{\wp_u^2} + U_3\sin U_4 \\ \vartheta(t') = U_3\left(\mu'\cos U_4 - E'\sin U_4\right) \end{cases} \quad (56)$$

Solving the system of equations (56) with respect to U_3 and U_4, we obtain:

$$U_3 = \frac{1}{\wp_u^2\mu'} \cdot \sqrt{\left(S(t')E' + \vartheta(t')\wp_u^2 - E'j_{sm}\right)^2 + \left(S(t')\wp_u^2 - j_{sm}\right)^2\mu'^2} \quad (57)$$

$$\sin U_4 = \frac{\left(S(t')\wp_u^2 - j_{Sm}\right)\mu'}{\sqrt{\left(\left(S(t')E' + \vartheta(t')\right)\wp_u^2 - E'j_{Sm}\right)^2 + \left(S(t')\wp_u^2 - j_{Sm}\right)^2\mu'^2}} \quad (58)$$

Similarly to equation (37) for σ we write the equation for:

$$\sigma' = \sigma_0' - m_3\frac{\left(E'^2 - \mu'^2\right)\sin(U_4 + \mu' t) - 2E'\mu'\cos(U_4 + \mu' t)}{\mu'\cos(U_4 + \mu' t) - E'\sin(U_4 + \mu' t)} \quad (59)$$

The load in the traction-coupling device for the section under consideration $t \geq t'$ is found similar to the load in the traction-coupling device of the section $0 \leq t \leq t'$ [20]

$$P_{pr} = j_{sm}(k_m - m_3)\left(1 + \frac{\wp_u}{\mu'}\right) \times \sqrt{\frac{\left[\left(S(t')E' + \vartheta(t')\right)^2 + \left(S(t')\right)^2\mu'^2\right]\wp_u^2}{j_{sm}^2} - \frac{2\left(S(t')\wp_u^2 + \vartheta(t')E'\right)}{j_{sm}} + 1} \cdot e^{-E't}\sin(U_4 + \mu' t). \quad (60)$$

$$P_d = \frac{j_{sm}}{\wp_u\mu'} \cdot \sqrt{\frac{\left[\left(S(t')E' + \vartheta(t')\right)^2 + \left(S(t')\right)^2\mu'^2\right]\wp_u^2}{j_{sm}^2} - \frac{2\left(S(t')\wp_u^2 + \vartheta(t')E'\right)}{j_{sm}} + 1} \cdot e^{-E't}\left[\begin{array}{l} 2E'\mu' k_m\cos(U_4 + \mu' t) - \\ -\left(2E'^2 k_m - \wp_u^2 m_3\right)\sin(U_4 + \mu' t)\end{array}\right] \quad (61)$$

Substituting equations (60, 61) into equation (38), we get:

$$P_{кг} = j_{sm}\left(\left(k_m - m_3\right) + \frac{k_m}{\wp_u\mu'}e^{-E't} \times \sqrt{\frac{\left[\left(S(t')E' + \vartheta(t')\right)^2 + \left(S(t')\right)^2\mu'^2\right]\wp_u^2}{j_{sm}^2} - \frac{2\left(S(t')\wp_u^2 + \vartheta(t')E'\right)}{j_{sm}} + 1} \times \left[\left(\mu'^2 - E'^2\right)\sin(U_4 + \mu' t) + 2E'\mu'\cos(U_4 + \mu' t)\right]\right) \quad (62)$$

Then the traction load peaks on this section will be calculated according to the following formula:

$$P_{кр\_e} = j_{sm}\left(\left(k_m - m_3\right) + k_m e^{-E't} \times \sqrt{\frac{\left[\left(S(t')E' + \vartheta(t')\right)^2 + \left(S(t')\right)^2\mu'^2\right]\wp_u^2}{j_{sm}^2} - \frac{2\left(S(t')\wp_u^2 + \vartheta(t')E'\right)}{j_{sm}} + 1}\right) \quad (63)$$

where:

$$t = \frac{1}{\mu}arctg\frac{\mu'\vartheta(t')\left(\mu'^2 - 3E'^2\right) + 2E'\mu'\left(j_{sm} - S(t')\wp_u^2\right)}{E'\vartheta(t')\left(3\mu'^2 - E'^2\right) + \left(E'^2 - \mu'^2\right)\left(j_{sm} - S(t')\wp_u^2\right)} \quad (64).$$

4. The Influence of the Design of the Traction Coupling Device on the Change in the Normal Reactions on the Tractor and Trailer Axles During Braking

Let's determine the normal reactions acting on the axle of the tractor and trailer during braking. And therefore, consider the system freely under the influence of active efforts and reactions of connections, replacing the action of connections with their reactions [15, 18, 19].

Normal reactions on the axles of the tractor and trailer are determined from the equation of the balance of forces acting on the transport-technological unit during braking.

On the front axle of the tractor:

$$N_1 = \frac{m_{tr} g a_2 + P_{in\_1} h_{tr} - P_{кг} h_c}{L_{ек}} \quad (65)$$

On the rear axle of the tractor:

$$N_2 = \frac{m_{tr} g a_1 - P_{in\_1} h_{tr} - P_{кк} h_c}{L_{tr}} \quad (66)$$

On the front axle of the trailer:

$$N_2 = \frac{m_{TP} g a_4 + P_{in\_2} h_{TP} - P_{кр} h_{сц}}{L_{ПР}} \quad (67)$$

On the rear axle of the trailer:

$$N_4 = \frac{m_{tr} g a_4 - P_{in\_2} h_{TP} - P_{кг} h_c}{L_{pr}} \quad (68)$$

Let's write down the forces of inertia of the links of the transport-technological unit during braking:

for a tractor

$$P_{in\_1} = N_2 \varphi + P_{кг}, \quad (69)$$

for trailer

$$P_{in\_2} = m_{ПР} g \varphi - P_{кр}, \quad (70)$$

Let's substitute the right parts of equations (83) and (70) into equations (67-70), we get:

for the front axle of the tractor

$$N_1 = \frac{m_{tr} g (a_2 + \varphi h_{tr}) - P_{кг} (h_c - h_{tr})}{L_{tr} + \varphi h_{tr}} \quad (71)$$

for the rear axle of the tractor

$$N_2 = \frac{m_{tr} g a_1 + P_{кг} (h_c - h_{tr})}{L_{tr} + \varphi h_{tr}} \quad (72)$$

for the front axle of the trailer

$$N_3 = \frac{m_{TP} g (a_4 + \varphi h_{TP}) + P_{кр} (h_{сц} - h_{TP})}{L_{TP}} \quad (73)$$

for the rear axle of the trailer

$$N_4 = \frac{m_{pr} g (a_3 - \varphi h_{tr}) - P_{кг} (h_c - h_{tr})}{L_{pr}} \quad (74)$$

Based on the calculations, the dependence of the normal reactions on the axles of the transport-technological unit on the braking efficiency (Fig. 2), the distance from the center of mass of the tractor to the line of action of the traction force (Fig. 3), taking into account the force in the connections of the traction-coupling devices and from the traction force (Fig. 4).

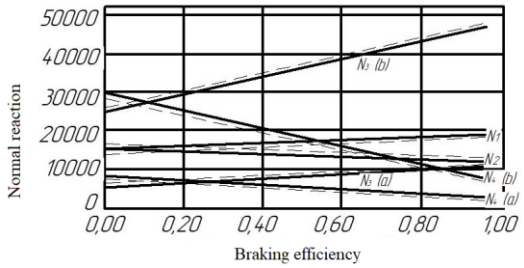

Figure 2: Dependence of normal reactions on the braking efficiency of the transport-technological train

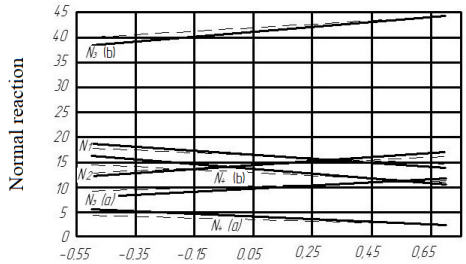

Figure 3: Dependence of normal reactions on the distance from the center of mass of the link to the line of action of the traction force

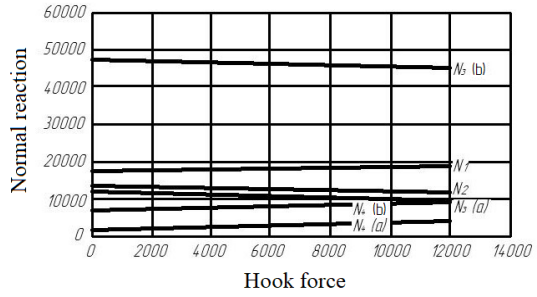

Figure 4: Dependence of normal reactions on traction force

5. Conclusions

Analyzing the dependences shown in (Fig. 3 and Fig. 4), it can be concluded that with the same braking forces, the coupling coefficient, the redistribution of normal reactions obtained due to a decrease in the amplitude of the traction force and its root mean square deviation due to the elastic properties of the traction-coupling device at the clutch point, creating a greater margin of lateral stability, thereby increasing the average speed of movement and safe initial braking speed and increasing the specific weight of the rear, which performs braking of this link of the tractor axle, thus increasing the braking qualities of the transport-technological train.

References

[1] Altomonte A., Frasci E., Di Ilio G., Arsie I., Jannelli E. Experimental testing of a heavy-duty Diesel engine at the dynamic test bench to assess the potential of regenerative braking. 2023 IEEE International Workshop on Metrology for Automotive, MetroAutomotive 2023 – Proceedings. 2023 3rd

IEEE International Workshop on Metrology for Automotive, MetroAutomotive 2023. Modena. 28 – 30 June 2023. p.p. 13 – 18.
[2] Rakha, H.; Yue, H.; Dion, F. VT-Meso model framework for estimating hot-stabilized light-duty vehicle fuel consumption and emission rates. Can. J. Civ. Eng. 2011, 38, p.p. 1274–1286.
[3] Tucki, K. A Computer Tool for Modelling CO2 Emissions in Driving Tests for Vehicles with Diesel Engines. Energies 2021, 14, p. 266.
[4] Felez J., Lopez-Mendez A. Advanced steering stability controls for articulated vehicles by using bond graphs and model predictive control. Simulation Series 53, №3, 2021. International Conference on Bond Graph Modeling and Simulation, ICBGM 2021. San Diego, 10 November 2021. p.p. 98 – 110.
[5] Borawski A. Effects of initial speed and load of universal semitrailer on braking system's friction pair heating. Heat Transfer Research Volume 51, Issue 15, 2020. p.p. 1417 – 1428.
[6] Samorodov V., Kozhushko A., Pelipenko E. Formation of a rational change in controlling continuously variable transmission at the stages of a tractor's acceleration and braking. Eastern-European Journal of Enterprise Technologies. 2016. Volume 4, Issue 7-82, p.p. 37-44.
[7] X. Shiwei, Z. Xiaopeng, J. Yuan, W. Lulu, H. Jingjing, Z. Xinyu Research on the Multi-Mode Composite Braking Control Strategy of Electric Wheel-Drive Multi-Axle Heavy-Duty Vehicles. World Electr. Veh. J. 2024, 15(3), 83.
[8] Ovsyannikov S., Kalinin E., Koliesnik I. Oscillation process of multi-support machines when driving over irregularities. International Scientific Conference Energy Management of Municipal Facilities and Sustainable Energy Technologies. Vol. 1. EMMFT. 2020. p.p. 307-317.
[9] W. Zhen, G. Feng, D. Jing, W. Xuelei Dynamics model and braking performance analysis of multi-axle vehicle. Zhongguo Jixie Gongcheng / China Mechanical Engineering. Volume 19, Issue 3, p.p. 365 – 369.
[10] W. Xinping, H. Rongnian, G. Han, C. Mengyu Electronic mechanical braking system executive mechanism design, calculation, and modeling based on dynamic control. Frontiers in Mechanical Engineering. Volume 10, 2024. DOI: 10.3389/fmech.2024.1368683.
[11] Cole, Colin & Spiryagin, Maksym & Wu, Qing & Sun, Y.. (2017). Modelling, simulation and applications of longitudinal train dynamics. Vehicle System Dynamics. 55. 1-74. 10.1080/00423114.2017.1330484. Kurka V. Force-measuring devices for machine-tractor units: Monograph / Kurka V., Linnik A., Bilyk S., Dinya V., Dubchak N., Semeniv I. - Kyiv: NUBiP of Ukraine, CPU "COMPRINT". 2019 – p. 192.
[12] Vicente, Bernardo & James, Sebastian & Anderson, Sean. (2020). Linear System Identification Versus Physical Modeling of Lateral-Longitudinal Vehicle Dynamics. IEEE Transactions on Control Systems Technology. PP. 1-8. 10.1109/TCST.2020.2994120.
[13] Y. Megantara, Tubagus & Supian, Sudradjat & Chaerani, Diah. (2024). Mathematical Modeling on Integrated Vehicle Assignment and Rebalancing in Ride-hailing System with Uncertainty Using Fuzzy Linear Programming. Journal of Advanced Research in Applied Sciences and Engineering Technology. 42. 133-144. 10.37934/araset.42.2.133144.
[14] Sadono, Aryo & Mahendra, Oka & Saputra, Roni & Rijanto, Estiko. (2024). Dynamics and control simulation of DC series motor for electric vehicle in regenerative braking. 10.1063/5.0205710.
[15] I. Koliesnik, E. Kalinin, I. Shevchenko, Ju. Koliesnik, O. Stepanov Conceptual Energy Model of the Dynamics of a Transport-Technological Unit for the Appearance of Two Drive Axles. Lecture Notes in Networks and Systems. 4th International Conference on Reliable Systems Engineering, ICoRSE 2024. Volume 1129 LNNS, 2024, Pages 314 – 327, doi: 10.1007/978-3-031-70670-7_27.
[16] Davidyan, Gabriel & Bortman, Jacob & Kenett, Ron. (2024). Development of an Operational Digital Twin of a Freight Car Braking System for Fault Diagnosis. Advanced Theory and Simulations. 7. 10.1002/adts.202301257.
[17] Tubagus Robbi Megantara, Sudradjat Supian, & Diah Chaerani. (2024). Mathematical Modeling on Integrated Vehicle Assignment and Rebalancing in Ride-hailing System with Uncertainty Using Fuzzy Linear Programming. Journal of Advanced Research in Applied Sciences and Engineering Technology, 42(2), 133–144. https://doi.org/10.37934/araset.42.2.133144
[18] Wang, Quan & Wang, Zhiwei & Mo, Jiliang & Wang, Ruichen & Wang, Kaiyun. (2022). Effect and Mechanism of Wheel–Rail Adhesion on Torsional Vibration and Stability of the Braking System. Tribology International. 179. 108182. 10.1016/j.triboint.2022.108182.
[19] Lebedev, A., Shuliak, M., Lebedev, S., Khalin, S., Haidai, T., Kholodov, A., Pirogov, V., & Shaposhnyk, V. (2024). Determining conditions for providing maximum traction efficiency of tractor as part of a soil tillage unit. Eastern-European Journal of Enterprise Technologies, Volume 1(1 (127), pp. 6-14, 2024. doi: https://doi.org/10.15587/1729-4061.2024.297902.
[20] Kozhushko, A., Tkachov, V., Mittsel, M. & Sokolik, S. (2024). Optimization of traction properties the electric tractor based on the simulation dlg-powermix test cycles. International Journal of Mechatronics and Applied Mechanics, 15, pp. 70–78, 2024. doi: https://doi.org/10.17683/ijomam/issue14.5.
[21] Cole, C., Spiryagin, M., Wu, Q., & Sun, Y. Q. (2017). Modelling, simulation and applications of longitudinal train dynamics. Vehicle System Dynamics, 55(10), 1498–1571. https://doi.org/10.1080/00423114.2017.1330484.
[22] Kozhushko, A., Pelypenko, Y., Kravchenko, S., Danylenko, V. Improving the Procedure for Modeling Low Frequency Oscillations of the Free Surface Liquid in a Tractor Tank. Eastern-European Journal of Enterprise Technologies, 122 (7), 2023, pp. 61-68. https://doi.org/10.15587/1729-4061.2023.277254.